Safe Sequential Path Planning Under Disturbances and Imperfect Information

Somil Bansal*, Mo Chen*, Jaime F. Fisac, and Claire J. Tomlin

***Abstract*— Multi-UAV systems are safety-critical, and guarantees must be made to ensure no unsafe configurations occur. Hamilton-Jacobi (HJ) reachability is ideal for analyzing such safety-critical systems; however, its direct application is limited to small-scale systems of no more than two vehicles due to an exponentially-scaling computational complexity. Previously, the sequential path planning (SPP) method, which assigns strict priorities to vehicles, was proposed; SPP allows multi-vehicle path planning to be done with a linearly-scaling computational complexity. However, the previous formulation assumed that there are no disturbances, and that every vehicle has perfect knowledge of higher-priority vehicles' positions. In this paper, we make SPP more practical by providing three different methods to account for disturbances in dynamics and imperfect knowledge of higher-priority vehicles' states. Each method has different assumptions about information sharing. We demonstrate our proposed methods in simulations.**

I. Introduction

Recently, there has been an immense surge of interest in using unmanned aerial systems (UASs) for civil purposes [1]–[4]. Many of these applications will involve unmanned aerial vehicles (UAVs) flying in urban environments. As a result, government agencies such as the Federal Aviation Administration (FAA) and National Aeronautics and Space Administration (NASA) of the United States are trying to develop new scalable ways to organize an air space in which potentially thousands of UAVs can fly together [5], [6].

One essential problem that needs to be addressed is how a group of vehicles in the same vicinity can reach their destinations while avoiding collision with each other. In some previous studies that address this problem, specific control strategies for the vehicles are assumed, and approaches such as induced velocity obstacles have been used [7]–[9]. Other researchers have used ideas involving virtual potential fields to maintain collision avoidance while maintaining a specific formation [10], [11]. Although interesting results emerge from these studies, simultaneous trajectory planning and collision avoidance were not considered.

Trajectory planning and collision avoidance problems in safety-critical systems have been studied using Hamilton-Jacobi (HJ) reachability analysis, which provides guarantees on the success and safety of optimal system trajectories [12]–[16]. In this context, one computes the reachable set, defined as the set of states from which the system can be driven to a target set. HJ reachability has been successfully used in applications involving systems with no more than two vehicles [13], [17]–[19]. However, HJ reachability cannot be directly applied to systems involving multiple vehicles due to its exponentially scaling computational complexity.

To overcome this problem, [20] presents sequential path planning (SPP), in which vehicles are assigned a strict priority ordering. In SPP, higher-priority vehicles ignore the lower-priority vehicles, which must take into account the presence of higher-priority vehicles by treating them as induced time-varying obstacles. Under this structure, computation complexity scales just *linearly* with the number of vehicles. In addition, a structure like this has the potential to flexibly divide up the airspace for the use of many UAVs; this is an important task in NASA's concept of operations for UAS traffic management [6].

The formulation in [20], however, ignores disturbances and assumes perfect information about other vehicles' trajectories. In presence of disturbances, a vehicle's state trajectory evolution cannot be precisely known *a priori*; thus, it is impossible to commit to exact trajectories as required in [20]. In such a scenario, a lower-priority vehicle needs to account for all possible states that the higher-priority vehicles could be in. To do this, the lower-priority vehicle needs to have some knowledge about the control policy used by each higher-priority vehicle. The main contribution of this paper is to take advantage of the computation benefits of the SPP scheme while resolving some of its practical challenges. In particular, we achieve the following:

- incorporate disturbances into the vehicle models,
- analyze three different assumptions on information to which lower-priority vehicles may have access,
- for each information pattern, propose a reachability-based method to compute the induced obstacles and the reachable sets that guarantee collision avoidance as well as successful transit to the destination.

II. Problem Formulation

Consider N vehicles, denoted $Q_i, i = 1, \ldots, n$, whose dynamics are described by the ordinary differential equation

$$\begin{aligned} \dot{x}_i &= f_i(t, x_i, u_i, d_i), \quad t \leq t_i^{\text{STA}} \\ u_i &\in \mathcal{U}_i, d_i \in \mathcal{D}_i, \quad i = 1, \ldots, N \end{aligned} \tag{1}$$

where $x_i \in \mathbb{R}^{n_i}$, u_i denote the state and control of ith vehicle Q_i respectively, and d_i denotes the disturbance experienced by Q_i. In general, the physical meaning of x_i and the dynamics f_i depend on the specific dynamic model of Q_i, and need not be the same across the different vehicles. t_i^{STA} in (1) denotes the scheduled time of arrival of Q_i.

For convenience, we will use the sets $\mathbb{U}_i, \mathbb{D}_i$ to denote the set of functions from which the control and disturbance

This work has been supported in part by NSF under CPS:ActionWebs (CNS-931843), by ONR under the HUNT (N0014-08-0696) and SMARTS (N00014-09-1-1051) MURIs and by grant N00014-12-1-0609, by AFOSR under the CHASE MURI (FA9550-10-1-0567). The research of J. F. Fisac has received funding from the "la Caixa" Foundation.

* Both authors contributed equally to this work. All authors are with the Department of Electrical Engineering and Computer Sciences, University of California, Berkeley. {somil, mochen72, jfisac, tomlin}@eecs.berkeley.edu

functions $u_i(\cdot), d_i(\cdot)$ can be drawn. Let $p_i \in \mathbb{R}^p$ denote the position of Q_i. Denote the rest of the states h_i, so that $x_i = (p_i, h_i)$. The initial state of Q_i is given by x_{i0}. Under the worst case disturbance, each vehicle aims to get to some set of target states, denoted $\mathcal{T}_i \subset \mathbb{R}^{n_i}$, by some scheduled time of arrival t_i^{STA}. On its way to $\mathcal{T}_i$, each vehicle must avoid the danger zones $\mathcal{A}_{ij}(t)$ of all other vehicles $j \neq i$ for all time. In general, the danger zone can be defined to capture any undesirable configurations between Q_i and Q_j. In this paper, we define $\mathcal{A}_{ij}(t)$ as

$$\mathcal{A}_{ij}(t) = \{x_i \in \mathbb{R}^{n_i} : \|p_i - p_j(t)\|_2 \leq R_c\} \tag{2}$$

the interpretation of which is that a vehicle is in another vehicle's danger zone if the two vehicles are within a Euclidean distance of R_c apart.

The problem of driving each of the vehicles in (1) into their respective target sets $\mathcal{T}_i$ would be in general a differential game of dimension $\sum_i n_i$. However, due to the exponential scaling of the complexity with the problem dimension, an optimal solution is computationally intractable even for $N > 2$, with n_i as small as 3.

In this paper, we assume that vehicles have assigned priorities as in the SPP method [20]. Since the analysis in [20] did not take into account the presence of disturbances d_i and limited information available to each vehicle, we extend the work in [20] to answer the following:

1) How can each vehicle guarantee that it will reach its target set without getting into any danger zones, despite the disturbances it and other vehicles experience?
2) How should each vehicle robustly handle situations with limited information about the state, control policy, and intention of other vehicles?

III. Background

This section provides a brief summary of [20], in which the SPP scheme is proposed under perfect information and absence of disturbances. Here, the dynamics of Q_i becomes

$$\begin{aligned} &\dot{x}_i = f_i(t, x_i, u_i), \quad t \leq t_i^{\text{STA}} \\ &u_i \in \mathcal{U}_i, \quad i = 1, \ldots, N \end{aligned} \tag{3}$$

where the difference compared to (1) is that the disturbance d_i is no longer a part of the dynamics.

In order to make the N-vehicle path planning problem safe and tractable, a reasonable structure is imposed to the problem: the vehicles are assigned a strict priority ordering. When planning its trajectory to its target, a higher-priority vehicle can disregard the presence of a lower-priority vehicle. In contrast, a lower-priority vehicle must take into account the presence of all higher-priority vehicles, and plan its trajectory in a way that avoids the higher-priority vehicles' danger zones. For convenience and without lost of generality, let Q_i be the vehicle with the ith highest priority.

Under the above convention, each vehicle Q_i must take into account time-varying obstacles induced by vehicles $Q_j, j < i$, denoted $\mathcal{O}_i^j(t)$ and represent the set of states that could possibly be in the danger zone of Q_j. Optimal safe path planning of each lower-priority vehicle Q_i then consists of determining the optimal path that allows Q_i to reach its target $\mathcal{T}_i$ while avoiding the time-varying obstacles $\mathcal{G}_i(t)$, defined by

$$\mathcal{G}_i(t) = \bigcup_{j=1}^{i-1} \mathcal{O}_i^j(t) \tag{4}$$

Such an optimal path planning problem can be solved by computing a backward reachable set (BRS) $\mathcal{V}_i(t)$ from a target set $\mathcal{T}_i$ using formulations of HJ variational inequalities (VI) such as [12], [14], [16], [21]. For example, to compute BRSs under the presence of time-varying obstacles, the authors in [21] augment system with the time variable, and then applied reachability theory for time-invariant systems. To avoid increasing the problem dimension and save computation time, for the simulations of this paper we utilize the formulation in [16], which does not require augmentation of the state space with the time variable.

Starting from the highest-priority vehicle Q_1, one computes the BRS $\mathcal{V}_1(t)$, from which the optimal control and trajectory $x_1(\cdot)$ to $\mathcal{T}_1$ can be obtained. Under the absence of disturbances and perfect information, obstacles induced by a higher-priority vehicle Q_j, starting with $j = 1$, for a lower-priority vehicle Q_i is simply the danger zone centered around the position $p_j(\cdot)$ of each point on the trajectory:

$$\mathcal{O}_i^j(t) = \{x_i : \|p_i - p_j(t)\| \leq R_c\} \tag{5}$$

Given $\mathcal{O}_i^j(t), j < i$, and continuing with $i = 2$, the optimal safe trajectories for each vehicle Q_i can be computed. All of the trajectories are optimal in the sense that given the requirement that Q_i must arrive at $\mathcal{T}_i$ by time t_i^{STA}, the latest departure time t_i^{LDT} and the optimal control $u_i^*(\cdot)$ that guarantees arrival by t_i^{STA} can be obtained.

To compute $\mathcal{V}_i(t)$ using the method in [16], we solve the following HJ VI for $t \leq t_i^{\text{STA}}$:

$$\begin{aligned} \max \Big\{ &\min \left\{ D_t V_i(t, x_i) + H_i\left(t, x_i, D_{x_i} V_i\right), \right. \\ &\left. l_i(x_i) - V_i(t, x_i) \right\}, -g_i(t, x_i) - V_i(t, x_i) \Big\} = 0 \\ &V_i(t_i^{\text{STA}}, x_i) = \max\left\{ l_i(x_i), -g_i(0, x_i) \right\} \end{aligned} \tag{6}$$

$$H_i\left(t, x_i, \lambda\right) = \min_{u_i \in \mathcal{U}_i} \lambda \cdot f_i(t, x_i, u_i) \tag{7}$$

where λ is the gradient of the value function, $D_{x_i} V_i$, and $l_i(x_i), g_i(t, x_i), V_i(t, x_i)$ are implicit surface functions representing the target $\mathcal{T}_i$, the time-varying obstacles $\mathcal{G}_i(t)$, and the backward reachable set $\mathcal{V}_i(t)$, respectively:

$$\begin{aligned} x_i \in \mathcal{T}_i &\Leftrightarrow l_i(x_i) \leq 0 \\ x_i(t) \in \mathcal{G}_i(t) &\Leftrightarrow g_i(t, x_i) \leq 0 \\ x_i(t) \in \mathcal{V}_i(t) &\Leftrightarrow V_i(t, x_i) \leq 0 \end{aligned} \tag{8}$$

The optimal control is given by

$$u_i^*\left(t, x_i\right) = \arg\min_{u_i \in \mathcal{U}_i} \lambda \cdot f_i(t, x_i, u_i) \tag{9}$$

IV. Disturbances and Incomplete Information

Disturbances and incomplete information significantly complicate the SPP scheme. The main difference is that the vehicle dynamics satisfy (1) as opposed to (3). Committing to exact trajectories is therefore no longer possible, since the disturbance $d_i(\cdot)$ is *a priori* unknown. Thus, the induced obstacles $\mathcal{O}_i^j(t)$ are no longer just the danger zones centered around positions. We present three methods to address the above issues. The methods differ in terms of control policy information that is known to a lower-priority vehicle about a higher-priority vehicle, and have their relative advantages and disadvantages depending on the situation. The three methods are as follows:

- **Centralized control**: A specific control strategy is enforced upon a vehicle; this can be achieved, for example, by some central agent such as an air traffic controller.
- **Least restrictive control**: A vehicle is required to arrive at its targets on time, but has no other restrictions.
- **Robust trajectory tracking**: A vehicle declares a nominal trajectory which can be robustly tracked.

In general, the above methods can be used in combination in a single path planning problem, with each vehicle independently having different control policies. Lower-priority vehicles would then plan their paths while taking into account the control policy information known for each higher-priority vehicle. For clarity, we will present each method as if all vehicles are using the same method of path planning.

For simplicity of explanation, we assume that no static obstacles exist. If static obstacles do exist, the time-varying obstacles $\mathcal{G}_i(t)$ simply become the union of the induced obstacles $\mathcal{O}_i^j(t)$ in (4) and the static obstacles.

A. Method 1: Centralized Control

The highest-priority vehicle Q_1 first plans its path by computing the BRS (with $i = 1$)

$$\begin{aligned}&\mathcal{V}_i(t) = \{x_i : \exists u_i(\cdot) \in \mathbb{U}_i, \forall d_i(\cdot) \in \mathbb{D}_i, x_i(\cdot) \text{ satisfies (1)},\\ &\forall s \in [t, t_i^{\text{STA}}], x_i(s) \notin \mathcal{G}_i(s), \exists s \in [t, t_i^{\text{STA}}], x_i(s) \in \mathcal{T}_i\}\end{aligned} \tag{10}$$

Since we have assumed no static obstacles exist, we have that for $Q_1, \mathcal{G}_1(s) = \emptyset\ \forall s \leq t_i^{\text{STA}}$, and thus the above BRS is well-defined. This BRS can be computed by solving the HJ VI (6) with the following Hamiltonian:

$$H_i(t, x_i, \lambda) = \min_{u_i \in \mathcal{U}_i} \max_{d_i \in \mathcal{D}_i} \lambda \cdot f_i(t, x_i, u_i, d_i) \tag{11}$$

where $l_i(x_i), g_i(t, x_i), V_i(t, x_i)$ are implicit surface functions representing the target $\mathcal{T}_i, \mathcal{G}_i(t), \mathcal{V}_i(t)$, respectively. From the BRS, we can obtain the optimal control

$$u_i^*(t, x_i) = \arg \min_{u_i \in \mathcal{U}_i} \max_{d_i \in \mathcal{D}_i} \lambda \cdot f_i(t, x_i, u_i, d_i) \tag{12}$$

Here, as well as in the other two methods, the latest departure time t_i^{LDT} is then given by $\arg\sup_t x_{i0} \in \mathcal{V}_i(t)$.

If there is a centralized controller directly controlling each of the N vehicles, then the control law of each vehicle can be enforced. In this case, lower-priority vehicles can safely assume that higher-priority vehicles are applying the enforced control law. In particular, the optimal controller for getting to the target, $u_i^*(t, x_i)$ can be enforced. In this case, the dynamics of each vehicle becomes

$$\begin{aligned}&\dot{x}_i = f_i^*(t, x_i, d_i) = f_i(t, x_i, u_i^*(t, x_i), d_i)\\ &d_i \in \mathcal{D}_i, \quad i = 1, \ldots, N, \quad t \in [t_i^{\text{LDT}}, t_i^{\text{STA}}]\end{aligned} \tag{13}$$

where u_i no longer appears explicitly in the dynamics.

From the perspective of a lower-priority vehicle Q_i, a higher-priority vehicle $Q_j, j < i$ induces a time-varying obstacle that represents the positions that could possibly be within the capture radius R_c of Q_j under the dynamics $f_j^*(t, x_j, d_j)$. Determining this obstacle involves computing a forward reachable set (FRS) of Q_j starting from $x_j(t_j^{\text{LDT}}) = x_{j0}$. The FRS $\mathcal{W}_j(t)$ is defined as follows:

$$\begin{aligned}&\mathcal{W}_j(t) = \{y \in \mathbb{R}^{n_j} : \exists d_j(\cdot) \in \mathbb{D}_j,\\ &x_j(\cdot) \text{ satisfies (13)}, x_j(t_j^{\text{LDT}}) = x_{j0}, x_j(t) = y\}\end{aligned} \tag{14}$$

The FRS can be computed using the following HJ VI:

$$\begin{aligned}&D_t W_j(t, x_j) + H_j\left(t, x_j, D_{x_j} W_j\right) = 0, t \in [t_j^{\text{LDT}}, t_j^{\text{STA}}]\\ &W_j(t_j^{\text{LDT}}, x_j) = \bar{l}_j(x_j)\\ &H_j(t, x_j, \lambda) = \max_{d_j \in \mathcal{D}_j} \lambda \cdot f_j^*(t, x_j, d_j)\end{aligned} \tag{15}$$

where $\bar{l}$ is chosen to be[1] such that $\bar{l}(y) = 0 \Leftrightarrow y = x_j(t_j^{\text{LDT}})$.

The FRS $\mathcal{W}_j(t)$ represents the set of possible states at time t of a higher-priority vehicle Q_j given all possible disturbances $d_j(\cdot)$ and given that Q_j uses the feedback controller $u_j^*(t, x_j)$. In order for a lower-priority vehicle Q_i to guarantee that it does not go within a distance of R_c to Q_j, Q_i must stay a distance of at least R_c away from the set $\mathcal{W}_j(t)$ for all possible values of the non-position states h_j. This gives the obstacle induced by a higher-priority vehicle Q_j for a lower-priority vehicle Q_i as follows:

$$\mathcal{O}_i^j(t) = \{x_i : \text{dist}(p_i, \mathcal{P}_j(t)) \leq R_c\} \tag{16}$$

where the $\text{dist}(\cdot, \cdot)$ function represents the minimum distance from a point to a set, and the set $\mathcal{P}_j(t)$ is the set of states in the FRS $\mathcal{W}_j(t)$ projected onto the states representing position p_j, and disregarding the non-position dimensions h_j:

$$\mathcal{P}_j(t) = \{p_j : \exists h_j, (p_j, h_j) \in \mathcal{W}_j(t)\}. \tag{17}$$

Finally, taking the union of the induced obstacles $\mathcal{O}_i^j(t)$ as in (4) gives us the time-varying obstacles $\mathcal{G}_i(t)$ needed to define and determine the BRS $\mathcal{V}_i(t)$ in (10). Repeating this process, all vehicles will be able to plan paths that guarantee the vehicles' timely and safe arrival.

B. Method 2: Least Restrictive Control

Here, we again begin with the highest-priority vehicle Q_1 planning its path by computing the BRS $\mathcal{V}_i(t)$ in (10). However, if there is no centralized controller to enforce the control policy for higher-priority vehicles, weaker assumptions must be made by the lower-priority vehicles to ensure collision avoidance. One reasonable assumption that a lower-priority vehicle can make is that all higher-priority vehicles

[1] In practice, we define the target set to be a small region around the vehicle's initial state for computational reasons.

follow the least restrictive control that would take them to their targets. This control would be given by

$$u_j(t,x_j) \in \begin{cases} \{u_j^*(t,x_j) \text{ given by (12)}\} \text{ if } x_j(t) \in \partial\mathcal{V}_j(t), \\ \mathcal{U}_j \text{ otherwise} \end{cases} \tag{18}$$

Such a controller allows each vehicle to use any controller, except when it is on the boundary of the BRS, $\partial\mathcal{V}_j(t)$, in which case $u_j^*(t,x_j)$ given by (12) must be used to get to the target safely and on time. This assumption is the weakest one that could be made by lower-priority vehicles given that the higher-priority vehicles will get to their targets on time.

Suppose a lower-priority vehicle Q_i assumes that higher-priority vehicles $Q_j, j < i$ use the least restrictive control strategy in (18). From the perspective of Q_i, a higher-priority vehicle Q_j could be in any state that is reachable from Q_j's initial state $x_j(t_j^{\text{LDT}}) = x_{j0}$ and from which the target $\mathcal{T}_j$ can be reached. Mathematically, this is defined by the intersection of a FRS from the initial state $x_j(t^{\text{LDT}}) = x_{j0}$ and the BRS defined in (10) from the target set $\mathcal{T}_j$, $\mathcal{V}_j(t) \cap \mathcal{W}_j(t)$. In this situation, since Q_j cannot be assumed to be using any particular feedback control, $\mathcal{W}_j(t)$ is defined as

$$\begin{aligned} \mathcal{W}_j(t) = \{&y \in \mathbb{R}^{n_j} : \exists u_j(\cdot) \in \mathbb{U}_j, \exists d_j(\cdot) \in \mathbb{D}_j, \\ &x_j(\cdot) \text{ satisfies (1)}, x_j(t_j^{\text{LDT}}) = x_{j0}, x_j(t) = y\} \end{aligned} \tag{19}$$

This FRS can be computed by solving (15) without obstacles, and with

$$H_j(t,x_j,\lambda) = \max_{u_j \in \mathcal{U}_j} \max_{d_j \in \mathcal{D}_j} \lambda \cdot f_j(t,x_j,u_j,d_j) \tag{20}$$

In turn, the obstacle induced by a higher-priority Q_j for a lower-priority vehicle Q_i is as follows:

$$\begin{aligned} \mathcal{O}_i^j(t) &= \{x_i : \text{dist}(p_i, \mathcal{P}_j(t)) \le R_c\}, \text{ with} \\ \mathcal{P}_j(t) &= \{p_j : \exists h_j, (p_j,h_j) \in \mathcal{V}_j(t) \cap \mathcal{W}_j(t)\} \end{aligned} \tag{21}$$

C. Method 3: Robust Trajectory Tracking

Although it is impossible to commit to and track an exact trajectory in the presence of disturbances, it may still be possible to *robustly* track a *nominal* trajectory with a bounded error at all times. If this can be done, then the tracking error bound can be used to determine the induced obstacles. Here, computation is done in two phases: the *planning phase* and the *disturbance rejection phase*. In the planning phase, we compute a nominal trajectory $x_{r,j}(\cdot)$ that is feasible in the absence of disturbances. In the disturbance rejection phase, we compute a bound on the tracking error.

In the planning phase, planning is done for a reduced control set $\mathcal{U}^p \subset \mathcal{U}$, as some margin is needed to reject unexpected disturbances while tracking the nominal trajectory. In the disturbance rejection phase, we determine the error bound independently of the nominal trajectory. Let x_j and $x_{r,j}$ denote the states of the actual vehicle Q_j and an arbitrary nominal trajectory, respectively, and define the tracking error $e_j = x_j - x_{r,j}$. When the error dynamics are independent of the absolute state as in (22) (and also (7) in [13]), we can obtain error dynamics of the form

$$\begin{aligned} &\dot{e_j} = f_{e_j}(e_j,u_j,u_{r,j},d_j), \\ &u_j \in \mathcal{U}_j, u_{r,j} \in \mathcal{U}_j^p, d_j \in \mathcal{D}_j, \quad t \le 0 \end{aligned} \tag{22}$$

To obtain bounds on the tracking error, we first conservatively estimate the error bound around any reference state $x_{r,j}$, denoted $\mathcal{E}_j = \{e_j : \|p_{e_j}\|_2 \le R_{\text{EB}}\}$, where p_{e_j} denotes the position coordinates of e_j and R_{EB} is a design parameter. We next solve a reachability problem with its complement $\mathcal{E}_j^c$, the set of tracking errors violating the error bound, as the target in the space of the error dynamics. From $\mathcal{E}_j^c$, we compute the following BRS:

$$\begin{aligned} \mathcal{V}_j^{\text{EB}}(t,0) = \{&y : \forall u_j(\cdot) \in \mathbb{U}_j, \exists u_{r,j}(\cdot) \in \mathbb{U}_j^p, \exists d_j(\cdot) \in \mathbb{D}_i, \\ &e_j(\cdot) \text{ satisfies (22)}, e_j(t) = y, \exists s \in [t,0], e_j(s) \in \mathcal{E}_j^c\}, \end{aligned} \tag{23}$$

where the Hamiltonian to compute the BRS is given by:

$$H_j^{\text{EB}}(e_j,\lambda) = \max_{u_j \in \mathcal{U}_j} \min_{u_{r,j} \in \mathcal{U}_j^p, d_j \in \mathcal{D}_j} \lambda \cdot f_{e_j}(e_j,u_j,u_{r,j},d_j). \tag{24}$$

Letting $t \to -\infty$, we obtain the infinite-horizon control-invariant set $\Omega_j := \lim_{t\to-\infty} \left(\mathcal{V}_j^{\text{EB}}(t,0)\right)^c$. If Ω_j is nonempty, then the tracking error e_j at flight time is guaranteed to remain within $\Omega_j \subseteq \mathcal{E}_j$ provided that the vehicle starts inside Ω_j and subsequently applies the feedback control law

$$\kappa_j(e_j) = \arg \max_{u_j \in \mathcal{U}_j} \min_{u_{r,j} \in \mathcal{U}_j^p, d_j \in \mathcal{D}_j} \lambda \cdot f_{e_j}(e_j,u_j,u_{r,j},d_j). \tag{25}$$

The induced obstacles by each higher-priority vehicle Q_j can thus be obtained by:

$$\begin{aligned} \mathcal{O}_i^j(t) &= \{x_i : \exists y \in \mathcal{P}_j(t), \|p_i - y\|_2 \le R_c\} \\ \mathcal{P}_j(t) &= \{p_j : \exists h_j, (p_j,h_j) \in \Omega_j + x_{r,j}(t)\}, \end{aligned} \tag{26}$$

where the "+" in (26) denotes the Minkowski sum.

Since each vehicle Q_j, $j < i$, can only be guaranteed to stay within Ω_j, we must make sure during the path planning of Q_i that at any given time, the error bounds of Q_i and Q_j, Ω_i and Ω_j, do not intersect. This can be done by augmenting the total obstacle set by Ω_i:

$$\tilde{\mathcal{G}}_i(t) = \mathcal{G}_i(t) + \Omega_i. \tag{27}$$

Finally, given Ω_i, we can guarantee that Q_i will reach its target $\mathcal{T}_i$ if $\Omega_i \subseteq \mathcal{T}_i$; thus, in the path planning phase, we modify $\mathcal{T}_i$ to be $\tilde{\mathcal{T}}_i := \{x_i : \Omega_i + x_i \subseteq \mathcal{T}_i\}$, and compute a BRS, with the control authority $\mathcal{U}_i^p$, that contains the initial state of the vehicle. Mathematically,

$$\begin{aligned} \mathcal{V}_i^{\text{rtt}}(t,t_i^{\text{STA}}) = \{&y : \exists u_i(\cdot) \in \mathbb{U}_i^p, x_i(\cdot) \text{ satisfies (3)}, \\ &\forall s \in [t,t_i^{\text{STA}}], x_i(s) \notin \tilde{\mathcal{G}}_i(s), \\ &\exists s \in [t,t_i^{\text{STA}}], x_i(s) \in \tilde{\mathcal{T}}_i, x_i(t) = y\} \end{aligned} \tag{28}$$

The Hamiltonian to compute $\mathcal{V}_i^{\text{rtt}}(t,t_i^{\text{STA}})$ and the optimal control for reaching $\tilde{\mathcal{T}}_i$ are given by (7) and (9) respectively. The nominal trajectory $x_{r,i}(\cdot)$ can thus be obtained by using vehicle dynamics (3), with the optimal control $u_i^{\text{rtt}}(\cdot)$. From the resulting nominal trajectory $x_{r,i}(\cdot)$, the overall control policy to reach $\mathcal{T}_i$ can be obtained via (25).

V. Numerical Simulations

We demonstrate our proposed methods using a four-vehicle example. Each vehicle has the following model:

$$\begin{aligned} \dot{p}_{x,i} &= v_i \cos\theta_i + d_{x,i} \\ \dot{p}_{y,i} &= v_i \sin\theta_i + d_{y,i} \qquad\qquad \underline{v} \le v_i \le \bar{v}, |\omega_i| \le \bar{\omega} \\ \dot{\theta}_i &= \omega_i + d_{\theta,i} \qquad\qquad \|(d_{x,i}, d_{y,i})\|_2 \le d_r, |d_{\theta,i}| \le \bar{d_\theta} \end{aligned}$$

where $p_i = (p_{x,i}, p_{y,i}), \theta_i, d = (d_{x,i}, d_{y,i}, d_{\theta,i})$ respectively represent Q_i's position, heading, and disturbances in the three states. The control of Q_i is $u_i = (v_i, \omega_i)$, where v_i is the speed of Q_i and ω_i is the turn rate; both controls have a lower and upper bound. For illustration purposes, we choose $\underline{v} = 0.5, \bar{v} = 1, \bar{\omega} = 1$; however, our method can easily handle the case in which these inputs differ across vehicles and cases in which each vehicle has a different dynamic model. The disturbance bounds are chosen as $d_r = 0.1, \bar{d_\theta} = 0.2$, which correspond to a 10% uncertainty in the dynamics.

The initial states of the vehicles are given as follows:

$$\begin{aligned} x_1^0 &= (-0.5, 0, 0), & x_2^0 &= (0.5, 0, \pi), \\ x_3^0 &= (-0.6, 0.6, 7\pi/4), & x_4^0 &= (0.6, 0.6, 5\pi/4). \end{aligned} \tag{29}$$

Each of the vehicles has a target set $\mathcal{T}_i$ that is circular in their position p_i centered at $c_i = (c_{x,i}, c_{y,i})$ with radius r:

$$\mathcal{T}_i = \{x_i \in \mathbb{R}^3 : \|p_i - c_i\| \le r\} \tag{30}$$

For the example shown, we chose $c_1 = (0.7, 0.2), c_2 = (-0.7, 0.2), c_3 = (0.7, -0.7), c_4 = (-0.7, -0.7)$ and $r = 0.1$. The setup of the example is shown in Fig. 1a.

Using the SPP algorithms presented, we obtain $t_i^{\text{LDT}}, i = 1, 2, 3, 4$ assuming $t_i^{\text{STA}} = 0$. Note that even though t_i^{STA} is assumed to be same for all vehicles in this example for simplicity, our method can easily handle the case in which t_i^{STA} is different for each vehicle.

For each proposed method of computing induced obstacles, we show the vehicles' entire trajectories (colored dotted lines), and overlay their positions (colored asterisks) and headings (arrows) at a point in time in which they are in relatively dense configuration. In all cases, the vehicles are able to avoid each other's danger zones (colored dashed circles) while getting to their target sets in minimum time. In addition, we show the evolution of the BRS over time for Q_3 (green boundaries) as well as the obstacles induced by the higher-priority vehicles (black boundaries).

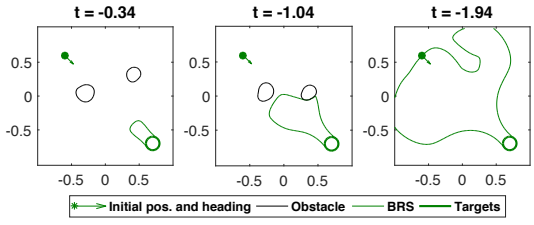

Fig. 2: Evolution of the BRS and the obstacles induced by Q_1 and Q_2 for Q_3 in the centralized control method.

Fig. 1b shows simulated trajectories in the situation where each vehicle uses $u_i^*(t, x_i)$ in (12). In this case, vehicles appear to deviate slightly from a straight line trajectory towards their targets, just enough to avoid higher-priority vehicles. The deviation is small since the centralized controller is quite

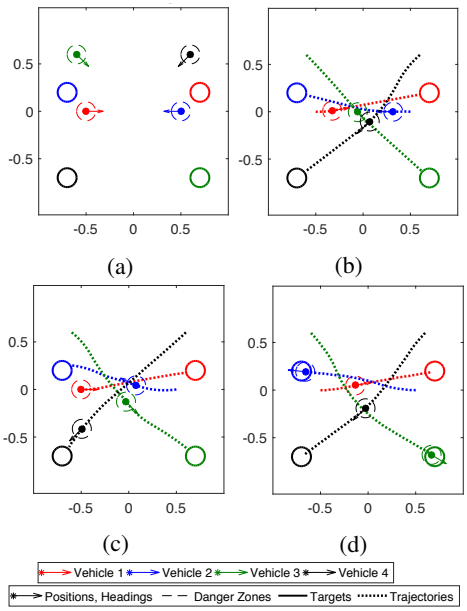

Fig. 1: Initial configuration and simulated trajectories of the vehicles for the three proposed methods.

restrictive, making the possible positions of higher-priority vehicles cover a small area. In the dense configuration at $t = -1.0$, the vehicles are close to each other but still outside each other's danger zones.

Fig. 2 shows the evolution of the BRS for Q_3 (green boundary), as well as the obstacles (black boundary) induced by the higher-priority vehicles. The size of the obstacles remains relatively small. t_i^{LDT} numbers for the four vehicles (in order) in this case are $-1.35, -1.37, -1.94$ and -2.04. They are relatively close for the vehicles, because the obstacles generated by higher-priority vehicles are small and hence do not affect t^{LDT} of the lower-priority vehicles significantly.

A. Least Restrictive Control

Fig. 1c shows the simulated trajectories in the situation where each vehicle assumes that higher-priority vehicles use the least restrictive control to reach their targets, as described in IV-B. Fig. 3 shows the BRS and induced obstacles for Q_3.

Q_1 (red) takes a relatively straight path to reach its target. From the perspective of all other vehicles, large obstacles are induced, since lower-priority vehicles make the weak assumption that higher-priority vehicles are using the least restrictive control. Because the obstacles induced are so large, it is optimal for lower-priority vehicles to wait until higher-priority vehicles pass. As a result, a dense configuration is never formed, and trajectories are relatively straight. The t_i^{LDT} values for vehicles are $-1.35, -1.97, -2.66$ and -3.39. Compared to the centralized control method, t_i^{LDT}'s decrease significantly except for Q_1, which need not account for any moving obstacles.

From Q_3's (green) perspective, the large obstacles induced by Q_1 and Q_2 are shown in Fig. 3 as the black boundaries. As the BRS (green boundary) evolves over time, its growth gets inhibited by the large obstacles for a long time, as evident

at $t = -0.89$. Eventually, the boundary of the BRS reaches the initial state of Q_3 at $t = t_3^{\text{LDT}} = -2.66$.

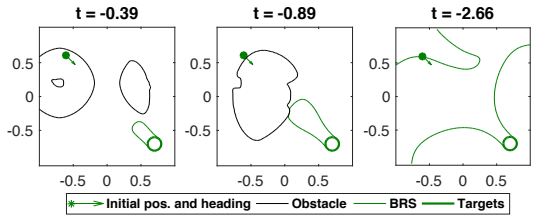

Fig. 3: Evolution of the BRS for Q_3 in the least restrictive control method. t_3^{LDT} is significantly lower than that in the centralized control method (-1.94 vs. -2.66).

B. Robust Trajectory Tracking

In the planning phase, we reduced the maximum turn rate of the vehicles from 1 to 0.6, and the speed range from $[0.5, 1]$ to exactly 0.75 (constant speed). With these reduced control authorities, we determined from the disturbance rejection phase that any nominal trajectory from the planning phase can be robustly tracked within a distance of 0.075.

Fig. 1d shows vehicle trajectories in the situation where each vehicle robustly tracks a nominal trajectory. Fig. 4 shows the BRS evolution and induced obstacles for Q_3.

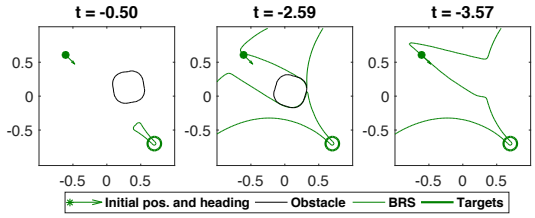

Fig. 4: Evolution of the BRS for Q_3 in the robust trajectory tracking method. Note that a smaller target set is used to ensure target reaching for any allowed tracking error.

In this case, the t_i^{LDT} values for the four vehicles are $-1.61, -3.16, -3.57$ and -2.47 respectively. In this method, vehicles use reduced control authority for path planning towards a reduced-size effective target set. As a result, higher-priority vehicles tend to have lower t^{LDT} compared to the other two methods, as evident from t_1^{LDT}. Because of this "sacrifice" made by the higher-priority vehicles during the path planning phase, the t^{LDT}'s of lower-priority vehicles may increase compared to those in the other methods, as evident from t_4^{LDT}. Overall, it is unclear how t_i^{LDT} will change for a vehicle compared to the other methods, as the conservative path planning increases t_i^{LDT} for higher-priority vehicles and decreases t_i^{LDT} for lower-priority vehicles.

VI. Conclusions

We have proposed three different methods to account for disturbances and imperfect control policy information in sequential path planning; these three methods can be used independently across the different vehicles in the path planning problem. In each method, different assumptions about the control strategy of higher-priority vehicles are made. In all of the methods, all vehicles are guaranteed to successfully reach their respective destinations without entering each other's danger zones despite the worst-case disturbance the vehicles could experience.

References

[1] W. M. Debusk, "Unmanned aerial vehicle systems for disaster relief: Tornado alley," in *Infotech@Aerospace Conferences*, 2010.

[2] Amazon.com, Inc. (2016) Amazon prime air. [Online]. Available: http://www.amazon.com/b?node=8037720011

[3] AUVSI News. (2016) UAS aid in south carolina tornado investigation. [Online]. Available: http://www.auvsi.org/blogs/auvsi-news/2016/01/29/tornado

[4] BBC Technology. (2016) Google plans drone delivery service for 2017. [Online]. Available: http://www.bbc.com/news/technology-34704868

[5] Jointed Planning and Development Office (JPDO), "Unmanned aircraft systems (UAS) comprehensive plan – a report on the nation's UAS path forward," Federal Aviation Administration, Tech. Rep., 2013.

[6] P. Kopardekar, J. Rios, T. Prevot, M. Johnson, J. Jung, and J. E. R. III, "UAS traffic management (UTM) concept of operations to safely enable low altitude flight operations," in *AIAA Aviation Technology, Integration, and Operations Conference*, 2016.

[7] P. Fiorini and Z. Shillert, "Motion planning in dynamic environments using velocity obstacles," *International Journal of Robotics Research*, vol. 17, pp. 760–772, 1998.

[8] G. C. Chasparis and J. S. Shamma, "Linear-programming-based multi-vehicle path planning with adversaries," in *Proceedings of American Control Conference*, June 2005.

[9] J. van den Berg, M. C. Lin, and D. Manocha, "Reciprocal velocity obstacles for real-time multi-agent navigation," in *IEEE International Conference on Robotics and Automation*, May 2008, pp. 1928–1935.

[10] R. Olfati-Saber and R. M. Murray, "Distributed cooperative control of multiple vehicle formations using structural potential functions," in *IFAC World Congress*, 2002.

[11] Y.-L. Chuang, Y. Huang, M. R. D'Orsogna, and A. L. Bertozzi, "Multi-vehicle flocking: Scalability of cooperative control algorithms using pairwise potentials," in *IEEE International Conference onRobotics and Automation*, April 2007, pp. 2292–2299.

[12] E. N. Barron, "Differential Games with Maximum Cost," *Nonlinear analysis: Theory, methods & applications*, pp. 971–989, 1990.

[13] I. Mitchell, A. Bayen, and C. Tomlin, "A time-dependent Hamilton-Jacobi formulation of reachable sets for continuous dynamic games," *IEEE Transactions on Automatic Control*, vol. 50, no. 7, pp. 947–957, July 2005.

[14] O. Bokanowski, N. Forcadel, and H. Zidani, "Reachability and minimal times for state constrained nonlinear problems without any controllability assumption," *SIAM Journal on Control and Optimization*, pp. 1–24, 2010.

[15] K. Margellos and J. Lygeros, "Hamilton-Jacobi Formulation for Reach-Avoid Differential Games," *IEEE Transactions on Automatic Control*, vol. 56, no. 8, Aug 2011.

[16] J. F. Fisac, M. Chen, C. J. Tomlin, and S. S. Shankar, "Reach-avoid problems with time-varying dynamics, targets and constraints," in *18th International Conference on Hybrid Systems: Computation and Controls*, 2015.

[17] J. Ding, J. Sprinkle, S. S. Sastry, and C. J. Tomlin, "Reachability calculations for automated aerial refueling," in *IEEE Conference on Decision and Control*, Cancun, Mexico, 2008.

[18] H. Huang, J. Ding, W. Zhang, and C. Tomlin, "A differential game approach to planning in adversarial scenarios: A case study on capture-the-flag," in *Robotics and Automation (ICRA), 2011 IEEE International Conference on*, 2011, pp. 1451–1456.

[19] A. M. Bayen, I. M. Mitchell, M. Oishi, and C. J. Tomlin, "Aircraft autolander safety analysis through optimal control-based reach set computation," *Journal of Guidance, Control, and Dynamics*, vol. 30, no. 1, 2007.

[20] M. Chen, J. Fisac, C. J. Tomlin, and S. Sastry, "Safe sequential path planning of multi-vehicle systems via double-obstacle hamilton-jacobi-isaacs variational inequality," in *European Control Conference*, 2015.

[21] O. Bokanowski and H. Zidani, "Minimal time problems with moving targets and obstacles," {*IFAC*} *Proceedings Volumes*, vol. 44, no. 1, pp. 2589 – 2593, 2011.